doi:10.26443/seismica.v3i1.386

Influence of outer-rise faults on shallow décollement heterogeneity and sediment flux at the Japan trench

E. Schottenfels [1], **C. Regalla** [*1], **Y. Nakamura** [2]

[1]School of Earth and Sustainability, Northern Arizona University, Flagstaff, AZ, USA, [2]Japan Agency for Marine-Earth Science and Technology (JAMSTEC), Yokosuka, Kanagawa, Japan

Author contributions: *Conceptualization*: E. Schottenfels, C. Regalla. *Data Curation*: Y. Nakamura. *Formal Analysis*: E. Schottenfels, C. Regalla. *Funding Acquisition*: C. Regalla. *Investigation*: E. Schottenfels. *Methodology*: E. Schottenfels. *Supervision*: C. Regalla. *Validation*: Y. Nakamura. *Visualization*: E. Schottenfels. *Writing – original draft*: E. Schottenfels. *Writing – review & editing*: E. Schottenfels, C. Regalla, Y. Nakamura.

Abstract We investigate the impact of outer-rise normal fault subduction on the structural evolution of the décollement and frontal prism in a portion of the Japan trench that hosted the 2011 Tohoku earthquake. We use seismic reflection data to map the relative occurrence of sediment accretion, sediment subduction, and frontal tectonic erosion in the shallow portion of the subduction zone and correlate these deformation styles to the magnitude of outer-rise fault throw and incoming plate sediment thickness. These data reveal spatial heterogeneity in the modes of deformation over distances of 5-10 km that necessitate correlative heterogeneity in the geometry and composition of the shallow décollement over similar length-scales. We find that sediment accretion predominantly occurs in regions where incoming plate sediment thickness is greater than fault throw. In these areas, the décollement appears to be non-planar and compositionally homogenous. Conversely, frontal tectonic erosion and slope failures are predominantly observed in regions where fault throw is greater than sediment thickness. In these areas, the décollement may be planar but compositionally heterogeneous. Additionally, spatial variations in near trench slip appear to correlate with the dominant deformation modes, suggesting that both sediment thickness and outer-rise fault throw may be important controls on shallow megathrust behavior.

Non-technical summary We investigate how properties of the subducting plate affect the structure of the shallow subduction zone off the coast of northern Japan, and how this may impact the earthquake potential of the region. We use geophysical reflection data to determine how sediment on top of the oceanic crust, and faults that displace the crust, can allow for sediment to be either scraped off or brought down into the subduction zone. We determine that these processes depend on both how thick the sediment is and how much displacement has occurred along faults. In areas where the sediment is thicker than the fault displacement, sediments are off-scraped and the interface between the upper and lower plate is more uniform in composition. In areas where the faults are larger than sediment thickness, the sediment is subducted, and the interface may have a varied composition. We identify variations in sediment and interface properties that have important implications for how the subduction zone evolves over time and for the style of shallow earthquakes. We suggest that the thickness of the sediment and the size of the faults on the subducting plate can help us understand such earthquake behavior.

Production Editor:
Gareth Funning
Handling Editor:
Randolph Williams
Copy & Layout Editor:
Hannah F. Mark

Signed reviewer(s):
Rebecca Bell
Harold Tobin

Received:
February 18, 2023
Accepted:
December 5, 2023
Published:
January 15, 2024

1 Introduction

The subduction of outer-rise normal faults is a nearly ubiquitous process that plays an important role in the mechanics of the shallow portion of the plate boundary fault (décollement) as lower plate surface roughness can modulate the frictional and fluid properties of the subduction interface (Clift and Vannucchi, 2004; Moore et al., 1986; Morgan et al., 2007; Polet and Kanamori, 2000; Saffer and Tobin, 2011; Tanioka et al., 1997). In many sediment-rich margins, this lower plate roughness is covered with a thick sediment sequence that often allows the décollement to "smooth over" the subducting topography (e.g., Contreras-Reyes et al., 2007; Wang and Bilek, 2014). In contrast, in sediment-poor margins, such as northeastern Japan, outer-rise normal faults produce significant offsets of the subducting oceanic crust and the seafloor outboard of the trench (e.g., Masson, 1991), which impart geometric and compositional heterogeneities that disrupt the continuity and evolution of the décollement (e.g., Polet and Kanamori, 2000; Tanioka et al., 1997). Constraints on the stratigraphic position and geometric evolution of the décollement are necessary for understanding the first-order control on the volumes of subducted versus accreted sediments, and the composition and strength of the shallow décollement (Saffer and Tobin, 2011; Moore et al., 2015; Polet and Kanamori, 2000). However, the factors controlling the evolution of the shallow décollement in response to subducting outer-rise faults remain unclear.

We evaluate how incoming plate sediment thickness

*Corresponding author: Christine.Regalla@nau.edu

and relief across outer-rise normal faults influence the evolution of the décollement and sediment fluxes at the shallow portion of the Japan trench. The Japan trench is a well-imaged margin that has become a type location for studies on outer-rise normal fault subduction and its impacts on sediment fluxes and forearc evolution (e.g., von Huene and Lallemand, 1990; Tanioka et al., 1997; von Huene and Culotta, 1989). Two different scenarios have been proposed for the evolution of the shallow portion of the subduction interface in northeastern Japan. In the first scenario, the development of a planar décollement across subducting horsts and grabens entraps both lower and upper plate sediments within subducted grabens and prevents voluminous sediment accretion (e.g., Hilde, 1983; von Huene et al., 1982; von Huene and Culotta, 1989). This model is supported by seismic reflection data that show sediment slumping into subducting grabens at the trench and a décollement that appears to project across lower plate grabens beneath the frontal prism (e.g., Hilde, 1983; Kodaira et al., 2012; Strasser et al., 2013). In the second scenario, the shallow décollement geometry mimics the subducted seafloor roughness, such that the majority of the incoming sediment section is offscraped and accreted (Nakamura et al., 2013; Regalla et al., 2019). This model is supported by high-resolution seismic reflection data (Nakamura et al., 2013, 2020) and drill cores collected across the plate boundary interface at the Japan trench (Chester et al., 2013) that show thrust imbrication of sediments near the trench and image an undulating décollement that appears to step over subducting horsts and grabens. Recently collected high-resolution seismic reflection data along the Japan trench show that both modes can occur along the margin (Nakamura et al., 2020). However, it remains unclear which processes control the evolution of the décollement in response to subducting horsts and grabens, the spatial variations in these processes along strike and down dip, and the relationship to the styles of slip along the shallow subduction interface.

Here, we analyze 44 seismic reflection profiles in a 40 x 180 km portion of the margin between 38°N and 40°N, in order to evaluate the relationship between sediment thickness, outer-rise fault throw, and modes of frontal prism deformation in a sediment-starved region that is known to be capable of hosting tsunamigenic slip (Figure 1). We calculate incoming plate sediment thickness and throw across normal faults on the incoming plate and beneath the prism, and identify modes of frontal prism deformation including sediment accretion, partial sediment accretion, complete sediment subduction, and frontal tectonic erosion. Our results show that the relative magnitudes of fault throw and sediment thickness together control modes of prism deformation, sediment flux, and shallow décollement heterogeneity. Sediment accretion is generally observed where sediment thickness is large relative to outer-rise fault throw, whereas frontal tectonic erosion occurs where fault throw is large relative to sediment thickness. These two styles of deformation have different endmember implications for the compositional and geometric heterogeneity of the shallow décollement that appear to correlate with different styles of shallow subduction interface slip. Therefore, sediment thickness and outer-rise fault throw may be important factors for predicting modes of frontal prism deformation, heterogeneity in the shallow subduction interface, and the conditions that may promote or inhibit shallow plate boundary slip.

2 Background

This study is performed along a portion of the NE Japan trench margin where high-density seismic reflection data allow for detailed evaluations of the frontal prism and incoming plate structure. At this location, the Pacific plate subducts beneath northern Honshu at a rate of ~80 mm/yr at the Japan trench (Seno et al., 1993) (Figure 1). The forearc consists of a high-velocity wedge (4-6 km/s P-wave) made of Cretaceous and younger accreted sediments (Tsuru et al., 2002; Kodaira et al., 2017), and a low velocity (2-3.5 km/s P-wave), seismically chaotic frontal prism, located at the seaward edge of the forearc. The prism is a wedge-shaped sedimentary package with a width of ~15–30 km that spans the margin parallel to the trench axis (Tsuru et al., 2002; Kodaira et al., 2017). The wedge appears to be composed of accreted incoming plate sediments derived from biogenic muds off-scraped from the incoming Pacific plate (Nakamura et al., 2013; Regalla et al., 2019), modified by large slope failures (Nakamura et al., 2020).

The incoming Pacific plate has a relatively thin sediment cover (~50–600 m) (Boston et al., 2014; Nakamura et al., 2023) due to limited biologic productivity in the north Pacific gyre and the relatively small volume of trench fill derived from the nearby continent and trench slopes (Moore et al., 2015; Ikehara et al., 2017). The incoming plate stratigraphy recovered at Deep Sea Drilling Project (DSDP) Leg 56/57 Site 436 (Figure 1) consists of basaltic crust overlain by ~100–160 m of Cretaceous to Oligocene chert, ~20–50 m of Eocene to early Miocene smectite-rich clay, and ~200–350 m of Miocene to Quaternary biogenic mud (Kodaira et al., 2020; Moore et al., 2015; Nakamura et al., 2013; Shipboard Scientific Party, 1980).

Flexure of the Pacific plate into the subduction zone generates bending-related normal faults that offset the oceanic crust and overlying sediments (e.g., Masson, 1991). Horsts and grabens bounded by these normal faults have widths of ~5–10 km and occur from the trench to ~120 km seaward of the trench axis. Fault offsets are ~100 m and increase towards the trench axis up to ~500 m (Boston et al., 2014). Horsts and grabens are also imaged beneath the upper plate up to 50 km landward of the trench axis, at depths up to 15 km, and with fault offsets up to 2 km (Tsuru et al., 2000; Kodaira et al., 2017). Some horsts and grabens on the incoming plate are associated with petit spot volcanism. Petit spot volcanoes are young (0–8 Ma) volcanic deposits, <300 m in height and <5 km in diameter, formed as a result of subduction-related plate flexure outboard of the trench axis (Hirano et al., 2006, 2019).

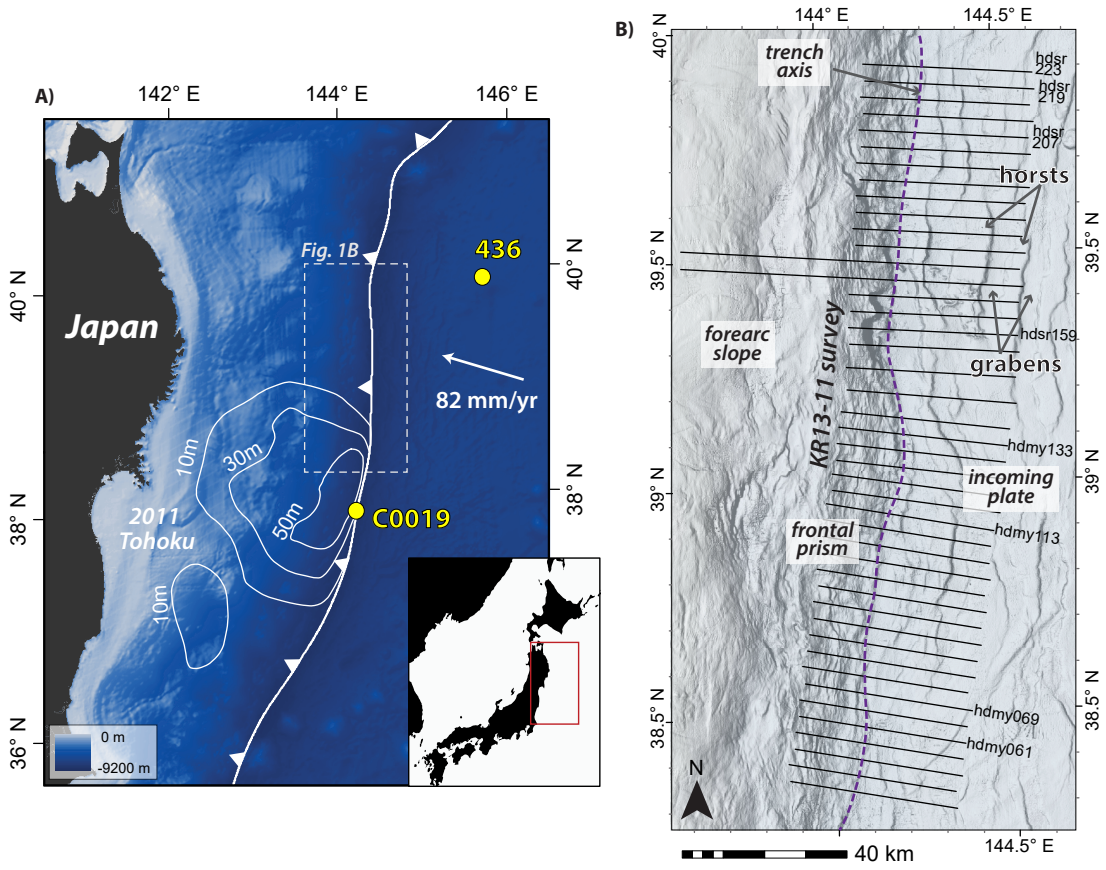

Figure 1 Location and tectonic setting of the study area at the Japan trench, offshore northeast Japan. **A.** Regional map showing the location of the trench, the plate convergence vector, and the M_w 9.0 2011 Tohoku earthquake rupture slip contours (white lines, after Iinuma et al., 2012). The study area (white dashed box, Figure 1b) is a ~40 km x 180 km region where 44 seismic reflection lines were collected by JAMSTEC (survey KR13-11). The survey area overlaps with the northern portion of the 2011 earthquake rupture. Locations of DSDP Site 436 and IODP Core C0019, which provide key stratigraphic data, are shown with yellow circles. **B.** Hillshaded 85 m DEM of the region in the white dashed box in panel A showing the trench axis (purple dashed line), forearc slope, frontal prism, and incoming plate horsts and grabens. Black lines show the locations of individual seismic reflection profiles mapped in this study.

3 Methods

We use 44 seismic reflection profiles that are 40 km in length and spaced ~4 km apart along the trench axis from ~38–40°N, collected and processed by the Japan Agency for Marine-Earth Science and Technology (JAMSTEC) (Figure 1). Lines were collected with Deep Sea Research Vessel *KAIREI* during the KR13-11 cruise using a cluster gun array with a volume of 380 in^3, 37.5 m shot interval, 6.25 m receiver interval, and a 1300 m-long streamer cable. The data are post-stack depth migrated lines. The velocity model used in the post-stack depth migration consists of three layers. The top layer is the water column and has a fixed velocity of 1525 m/s. The second layer is the soft sedimentary layer (SU1 and SU2). The velocity of the top of this layer is 1600 m/s and is linearly increased down to the bottom of this layer, with a 0.5 (m/s)/m gradient (namely, 1800 m/s at 400 m below seafloor, 2000 m/s at 800 m below seafloor). The model of the second layer was determined by comparing post-stack depth migrated profiles with several different gradient values. The gradient 0.5 (m/s)/m was chosen as it generated the best migrated image. The third layer is the chert and basement units (SU3 and SU4) and has a fixed velocity of 3000 m/s. We use these depth-migrated seismic reflection profiles to map seismic units (SUs) and faults, and to calculate sediment thickness and fault throw.

3.1 Seismic line mapping

We map seismic units on the incoming and overriding plate in the study area using the seismic stratigraphy of Nakamura et al. (2013, 2020, 2023) (Figure 2a). This work defines four seismic units (SU1 though SU4) based on seismic characteristics and correlations to known seismic and lithostratigraphic units of DSDP Site 436 and International Ocean Drilling Program (IODP) Expedition 343 Core C0019 (Nakamura et al., 2013). Seismic unit SU1, located landward of the trench, is an acoustically chaotic unit containing weak, discontinuous reflections. This unit is interpreted as the older, deformed equivalent of off-scraped incoming plate sediments (Nakamura et al., 2013, 2020; Regalla et al., 2019). Seismic unit SU2, located on the incoming plate and in frontal thrusts of the frontal prism, contains subhorizontal, parallel reflections with weak amplitudes. This unit is correlative to incoming plate sediments

composed of diatomaceous muds with a basal pelagic clay layer (Nakamura et al., 2013). We include trench fill deposits, parallel and continuous reflections that overly the incoming plate sediments near the deformation front, as part of the SU2 map unit (Nakamura et al., 2023). Seismic unit SU3 contains high amplitude, sub-horizontal, semi-continuous reflections and is correlated to a chert layer stratigraphically below SU2. Seismic unit SU4 contains high amplitude reflections that become more discontinuous and weaker amplitude with depth. This unit is correlated to the basaltic crust of the incoming plate underlying SU3 (Figure 2a).

We identify faults in the incoming and overriding plate where there is folding, truncation, or offset of parallel reflectors in seismic units, or where high amplitude reflectors truncate at seismic unit boundaries or the seafloor. We map three categories of faults: imbricate thrust faults in the frontal prism, the shallow plate boundary décollement, and normal faults that offset seismic units in the incoming plate. Imbricate thrust faults are identified as low angle (<30°) thrust faults that sometimes appear as high amplitude reflections separating repeating packages of SU2 in the frontal prism (Figures 3a and b and S1). These imbricate thrust faults sole into the décollement or higher in the sediment section. The décollement is a high-amplitude, semi-continuous reflection that separates undeformed strata in the subducting plate from deformed material in the overriding plate (Nakamura et al., 2013, 2020). Prior mapping demonstrates that the décollement is localized within SU1 or within or at the base of SU2 and is generally parallel to the top of the SU3 and SU4 units in the subducting plate (Nakamura et al., 2013, 2020). Normal faults on the incoming plate and subducting plate beneath the prism are identified based on truncation of units SU2, SU3, and SU4 where they are offset at a high angle (>50°) by landward or seaward dipping faults (e.g., Boston et al., 2014; Nakamura et al., 2023).

We also map petit spot volcanic deposits on the incoming plate, slope failures at the toe of the frontal prism, and the position of the deformation front at the trench axis. Petit spot volcanic deposits are identified as mounds or knolls with discontinuous, high amplitude seismic reflections that disturb the top of the oceanic crust and sediment section (Fujiwara et al., 2007; Fujie et al., 2020). Slope failures are identified based on the presence of steep, arcuate topographic slopes and associated mass transport deposits (Nakamura et al., 2020). The deformation front is mapped at the position where deformed frontal prism sediments intersect the undeformed sediments of the incoming plate. We infer the position of the deformation front where slope failures modify the frontal prism.

3.2 Incoming plate sediment thickness and normal fault throw

We measured the thickness of incoming plate sediments at multiple locations on each seismic reflection profile (Figure 1) to determine the thickness of sediment available for accretion. Prior seismic mapping, core, and borehole data indicate that the biogenic muds and clays of seismic unit SU2 can be accreted to the upper plate, whereas the more strongly lithified cherts of seismic unit SU3 appear to evade accretion and are largely subducted (e.g., Nakamura et al., 2013, 2020; Chester et al., 2013). We therefore calculate the incoming plate sediment thickness within SU2 as a proxy for the total thickness of sediment available for accretion. Here, the term "incoming plate sediment thickness" refers to the biogenic muds and pelagic clays of SU2 and does not include the cherts of SU3.

We define the thickness of SU2 as the distance between the top of the upper most strong reflection of SU3 and the reflection at the top of SU2 at the seafloor (Figure 2b). We measure apparent sediment thickness as the vertical distance between these two reflectors, then convert to true sediment thickness using local strata dip. Measurement locations were selected at sites that minimized the impacts of local sediment re-distribution and alteration. Specifically, we chose locations that are >1 kilometer away from either outer-rise faults, which generate local sediment erosion and redistribution; or petit spot volcanism, that can locally alter sediment thickness or composition.

We quantified outer-rise fault offset by measuring the vertical separation of stratigraphic units across normal faults by projecting offset horizons to the fault midpoint (Figure 2c). We chose to measure vertical separation rather than fault throw because fault throw can only be accurately measured when there are discrete faults with distinct stratigraphic cutoffs imaged in the seismic reflection profile. However, steeply dipping fault planes and stratigraphic cutoffs are rarely clearly imaged in the seismic reflection data (e.g., Figures S3-8). In contrast, vertical separation of offset layers can be measured even if a fault plane or cutoff cannot be directly imaged, because the offset stratigraphic horizons can be projected into the fault zone (Figure 2c). In this study area, vertical separation and fault throw agree to within +/- 50 m (calculated for fault dips >50° and strata dips of <5°).

We calculated vertical separation of the top of unit SU3 because the cherts of SU3 were deposited prior to the onset of outer-rise faulting, and therefore record total fault slip. We measured vertical separation of SU3 at locations where the horizon is clearly imaged and where unit truncations have well constrained positions. These selection criteria allowed us to measure vertical separation at two to four faulted locations per profile on the incoming plate outboard of the trench, and up to three locations on the subducted plate under the frontal prism.

We ranked the confidence of each vertical separation measurement from 1 (low) to 3 (high) based on the distinctness of the fault plane and stratigraphic cutoffs. For example, sites with a high confidence include a single, discrete, fault with clear cutoffs, whereas sites that contain multiple faults or have unclear unit truncations have low confidence. We then calculated weighted averages of fault throw using the following equation:

$$W = \frac{\sum \int_{i=1}^{n} w_i X_i}{\sum \int_{i=1}^{n} w_i} \quad (1)$$

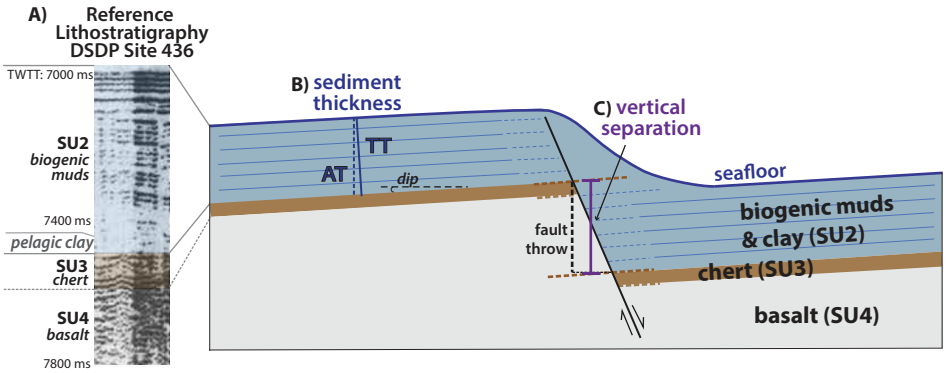

Figure 2 Schematic diagram of the incoming plate on a seismic line showing our approach to mapping seismic units (SUs), quantifying vertical separation (fault throw), and measuring sediment thickness. **A.** Seismic units (SUs) were mapped based on established correlations to known seismic and lithostratigraphic units of DSDP drill core at site 436 and to prior mapping of the margin (Nakamura et al., 2013, 2020; Nasu et al., 1980). See Section 3.1 for descriptions. **B.** Schematic diagram of a normal fault offsetting the incoming plate. True sediment thickness (TT) is calculated from apparent sediment thickness (AT), measured as the vertical depth difference between the seafloor reflection and the strong reflection of SU3 (chert), and the local dip of the strata. The dark blue line represents the seafloor reflection, which has the shape of a diffuse curve across the fault due to sediment redistribution and onlapping during fault slip. Reflectors within SU2 and SU3 are dashed where poorly resolved. **C.** Fault throw is determined by measuring the vertical separation of the chert horizon (SU3) across the fault by projecting the top of SU3 on the upthrown and downthrown blocks into the plane of the fault and calculating the vertical depth difference at the fault midpoint.

where W is the weighted average, w_i is site confidence weight, and X_i is site vertical separation. This approach allows us to identify spatial trends in normal fault throws that are most dependent on our highest confidence measurements.

4 Results

4.1 Seismic units and structure

4.1.1 Properties of the incoming plate outboard of the trench

Three seismic units are present on the incoming plate in the map area: SU2, SU3, and SU4. SU4 (basaltic crust) is mapped everywhere on the incoming plate outboard of the deformation front (Figures 3 and 4). SU3 and SU2 (chert, clay, and biogenic muds) are present nearly everywhere above SU4 on the incoming plate, except in regions where petit spot volcanic deposits are present. Petit spot volcanoes mapped in seismic reflection data are ~1–5 km in length and ~100–500 m in height (Figure 3e). There are three main clusters of petit spot volcanic deposits located at 39.25°N–39.75°N, 38.7°N–38.9°N, and possibly at 38.4°N (Figure 5).

Incoming plate sediment thickness varies between ~50 and 400 m, with more than half of the measured sites having thicknesses of 250–400 m (Figure 5a). There are, however, two ~20 x 20 km regions of anomalously thin (~50–200 m) sediments located at ~39.5°N and ~38.75°N. These regions are located near mapped locations of petit spot volcanism, where SU2 is thin or absent (e.g., Figure 3e). This spatial correlation between thin sediments and petit spot volcanism has been suggested to be a result of volcanic intrusions that metamorphose and effectively thin the muds and clays of the sediment section (e.g., Fujie et al., 2020; Hirano et al., 2006). The thin sediment regions we map are surrounded by ~10 km wide margins with intermediate sediment thicknesses (~200–300 m), and transition into "background" sediment thicknesses (250–400 m) over distances of ~>50 km.

Outer-rise faults offset seismic units SU2, SU3, and SU4 throughout the study area (Figures 4 and 5b). Normal faults outboard of the trench have strikes that are subparallel to the trench and are present from 0 to >100 km. Both landward and seaward dipping normal faults are present and bound networks of horsts and grabens. Normal faults have throws of ~90 m to 900 m, and generally increase in magnitude with proximity to the trench, in agreement with the findings of Boston et al. (2014). We note that there is one 20 km long region on the incoming plate at 39.4°N that contains a cluster of normal faults with very high fault throw (>300 m). This region is located in the vicinity of the petit spot volcanism around ~39.5°N (Figure 5b).

4.1.2 Properties of the subducted plate under the frontal prism

Seismic units SU4, SU3, and SU2 are also present under the frontal prism. SU4 (basaltic crust) is mapped everywhere on the subducted plate beneath the frontal prism (Figures 3 and 4). SU3 can be only definitively mapped under the frontal prism to within <~5 km of the deformation front, at which point the resolution of the seismic data often precludes separation of SU4 from SU3 (Figure 4). SU2 is typically not present on the subducting plate under the frontal prism, except at limited locations where it is present in subducted grabens (Figure 3b and d) or is underthrust beneath the frontal prism (Figure 3c).

We mapped subducted normal faults landward of the

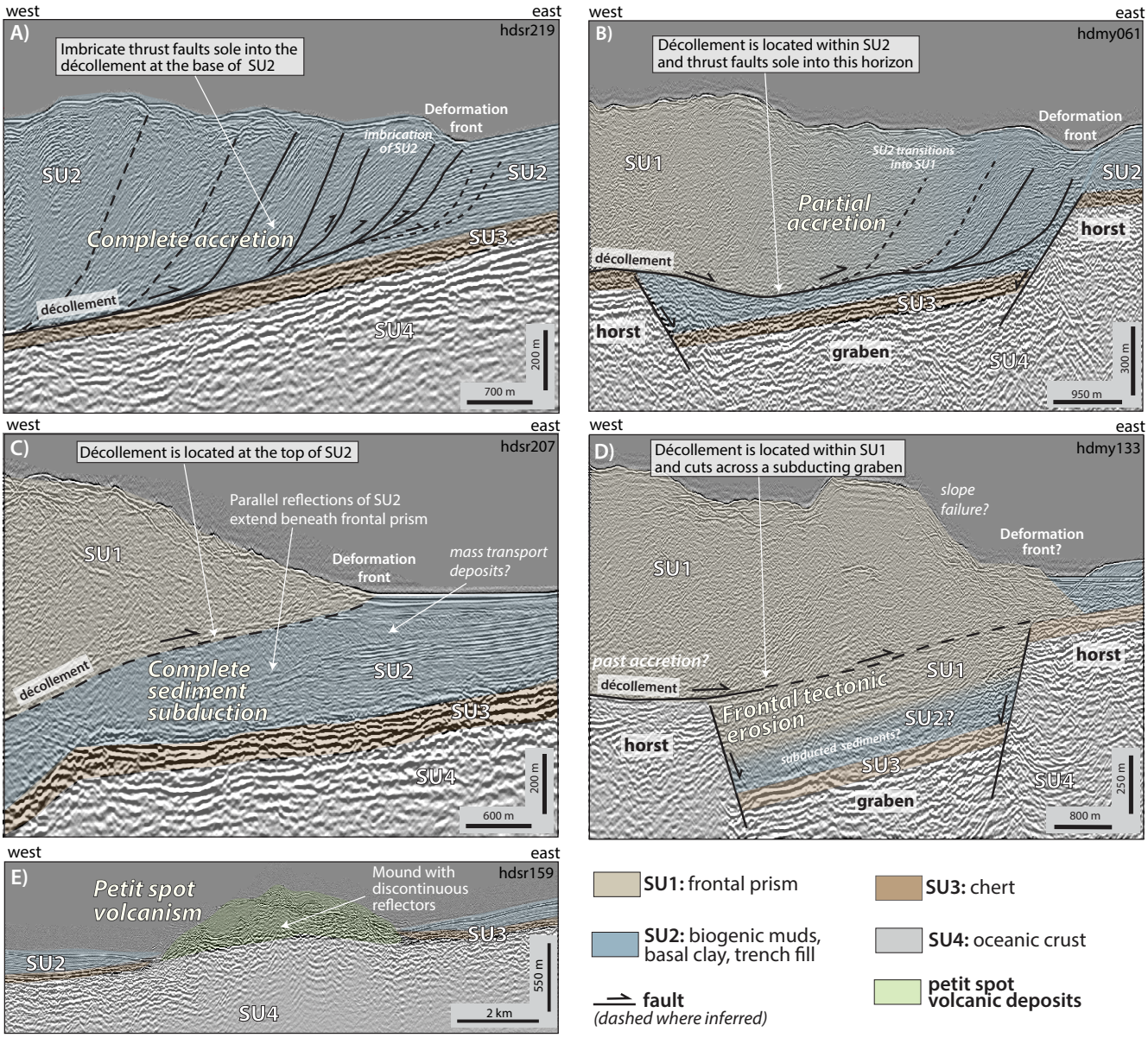

Figure 3 Annotated seismic lines showing examples of mapped seismic units, normal faults, imbricate thrust faults, and décollement position (see Supporting Information Figure S1 for non-annotated images). **A.** Example of a location where imbricate thrust faults in SU2 sole into the décollement at the base of SU2 (biogenic mud). We interpret this geometry to indicate that all SU2 sediments are accreted at the deformation front and SU3 and SU4 are locally subducted. **B.** Example of a location where imbricate thrust faults sole into décollement within SU2, rather than at its base. We interpret this geometry to represent partial sediment accretion, where SU2 above the décollement is accreted and SU2, SU3, and SU4 below are subducted. **C.** Example showing the décollement at the top of SU2 such that there is complete sediment subduction of units SU2, SU3, and SU4 beneath the frontal prism (SU1). **D.** Example of a location where the décollement appears to cut across SU1 to connect the tops of two horsts. Also note the steeply dipping slope at the deformation indicative of slope failure. We interpret this décollement geometry to indicate that part of SU1, and likely all of SU2, SU3, and SU4, are locally subducted. This geometry may lead to frontal tectonic erosion of prism sediments (e.g., Hilde, 1983). **E.** Example of petit spot volcanism on the incoming pate. Petit spot volcanoes are identified as seismically chaotic mounds (light green) that intrude and disrupt the oceanic crust and sediment section.

deformation front (under the frontal prism) and interpolated fault boundaries between adjacent seismic lines (Figure 5b). Normal faults subducted beneath the frontal prism branch and merge along strike and bound horsts and grabens that have length and widths comparable to that on incoming plate (Figure 5b and c). In some locations, the displacement along normal faults decreases along strike such that there are neither horsts nor grabens present in a line segment. These likely represent regions where there is flat subducting topography or relay ramps between adjacent faults. The average throw on normal faults under the frontal prism is 354 ± 163 m. This magnitude of offset is greater than the average throw on outer-rise faults outboard of the trench (261 ± 103 m), and implies that there is a continued accumulation of slip on normal faults following

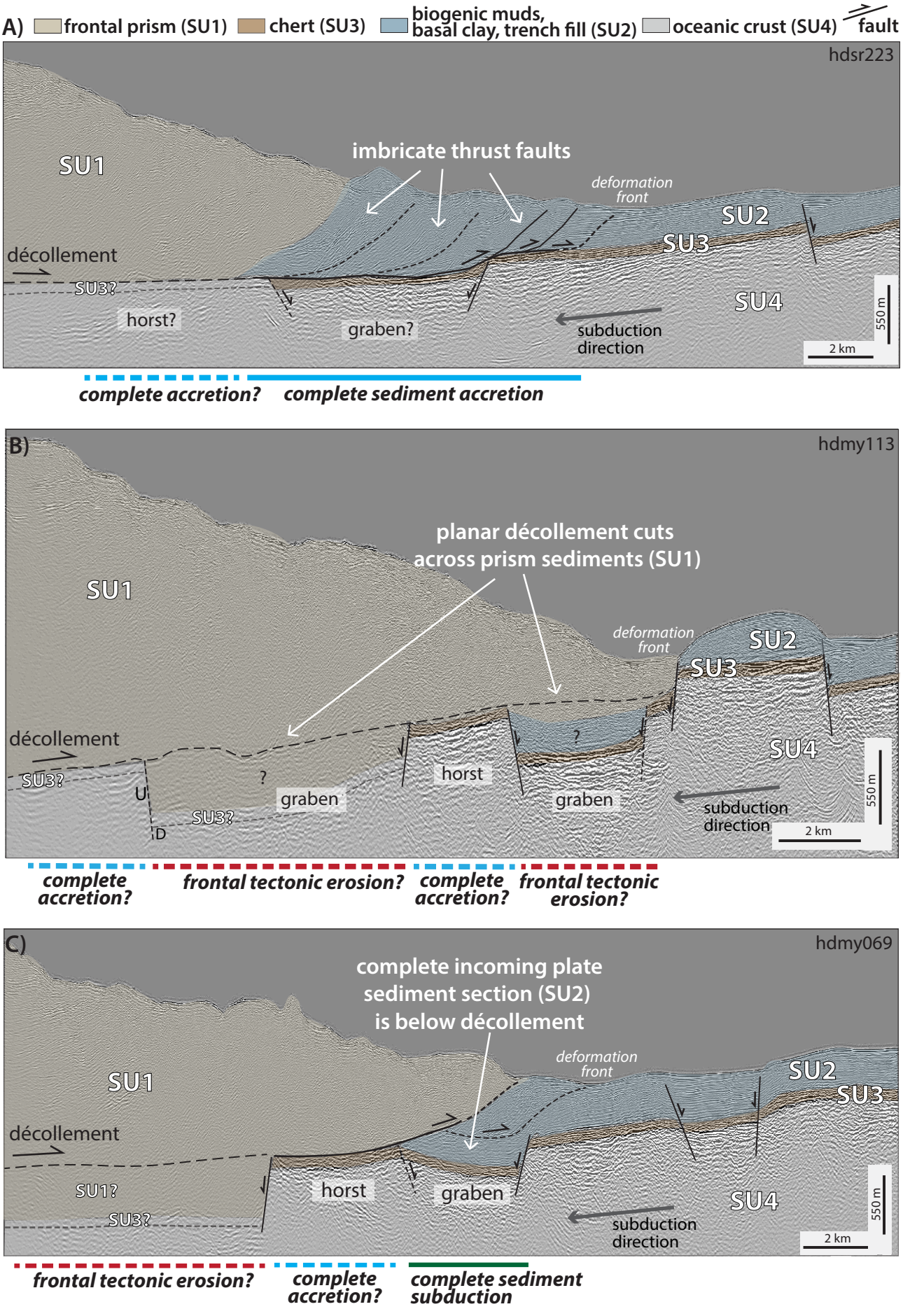

Figure 4 Caption on next page.

Figure 4 Examples of variations in mapped deformation modes, sediment flux, and décollement position within a seismic reflection profile. See Figures 1 and 5 for profile locations and the Supporting Information figures S3 – 5 for un-annotated versions of these seismic profiles. Inferred position of SU3 is shown as dashed lined on the landward portions of the profiles. **A.** Line hdsr223 has a single mode of deformation along the entire seismic profile. There is complete sediment accretion near the deformation front and inferred sediment accretion along landward segments. **B.** Line hdmy113 has two modes of deformation, alternating between frontal tectonic erosion within subducted grabens and sediment accretion on horsts. **C.** Line hdmy069 has three modes of deformation: complete sediment subduction near the deformation front, possible sediment accretion on the horst top, and potential tectonic erosion in the landward-most half-graben.

subduction under the frontal prism.

4.1.3 Properties of the overriding plate

Two seismic units are present in the overriding plate: SU1 (chaotic frontal prism) and deformed SU2 (biogenic muds and clay) (Figures 3 and 4). Unlike many margins with well-formed accretionary prisms, at the Japan trench it is difficult to resolve coherent reflectors within the frontal prism or identify internal deformation structures within SU1 (Nakamura et al., 2013, 2020). In contrast, where SU2 is present in the overriding plate, coherent reflectors are deformed into fault-related folds as the incoming sediments are repeated in imbricate thrusts that sole into a local décollement (Figure 3a and b). Imbricate thrust faults repeating SU2 are present in ~2/3 of the mapped seismic lines and comprise the outermost portion of the frontal prism (Figures 3a and b; 4a and c). In the other ~1/3 of the lines, SU1 is present all the way to the deformation front (Figures 3c and d; 4b). The nature of the boundary between SU1 and SU2 varies among seismic lines and can either be gradational (e.g., Figure 3b) or abrupt (e.g., Figure 4a).

In some locations, the internal structure of the prism is disrupted by slope failures that have heights of ~500 m–1 km and headwall slopes of ~20–30° (Figure 3d). The highest density of large slope failures occurs in a region between 39.3°N and 39.6°N (Figure 5c), inboard of a region on the incoming plate with very large offset outer-rise faults, thin sediments, and petit spot volcanism. This correlation suggests that slope failures may be promoted by the subduction of crust with large fault throw, thin sediment, and seafloor roughness generated by volcanism.

4.1.4 Properties of the décollement

The décollement in our study area is expressed in three ways: 1) a subhorizontal fault into which imbricate thrusts sole, 2) a high amplitude, subhorizontal reflector below SU1 and/or SU2 (Nakamura et al., 2013, 2020), or 3) the contact between SU1/SU2 and the underthrust units (Figure 3a-d). In locations where imbricate thrust faults sole into the base of SU2 at its contact with SU3 (Figure 3a), the décollement is likely hosted within a layer of smectite rich, frictionally weak clays (e.g., Chester et al., 2013; Kirkpatrick et al., 2015; Moore et al., 2015; Nakamura et al., 2013). Where the décollement is located within SU2 (Figure 3b), it is likely hosted within frictionally stronger biogenic muds (Ikari et al., 2015; Sawai et al., 2017).

High amplitude décollement reflectors mapped at depth may project into imbricate faults within the lower portion of SU2 (Figure 3a and b), or may project above SU3 and SU2, below SU1 (Figure 3c and d). Mapped décollement reflectors have two endmember geometries: a semi-planar trajectory across both horsts and graben (Figure 3d), or a non-planar geometry where it either steps down from a horst into a graben or steps up from graben into a horst (Figure 3b). The strength of the décollement reflector often changes as the décollement crosses into different seismic units. For example, a planar décollement that crosses from a horst top into prism sediment above a graben weakens in seismic character, whereas the décollement often maintains its seismic character as it steps down into a subducting graben (Figures 3 and S3-5).

In locations where there are neither imbricate thrust faults nor a clear high amplitude reflector, we infer the location of the décollement to be the position that separates SU1/SU2 material in the frontal prism from material on the subducted plate (Figure 3c and d), and it is inferred to have a position that is congruent with the décollement as mapped in the up-dip and down-dip directions. The unit or units present under the décollement vary as a function of distance from the trench, and as a function of its position relative to a subducted horst or graben. SU2 is mapped under the décollement in lines where some or all of the SU2 section is underthrust at the deformation front (Figure 3b and c) or at locations where SU2 is entrapped within a subducting graben (Figure 4c). Where SU2 is present under the décollement, it is usually undeformed and contains flat parallel reflectors (Figure 3b and c). Greater than ~1–3 km from the deformation front, the décollement typically separates SU1 in the overriding plate from SU3 or SU4 in the downgoing plate (Figure 4b and c), and SU2 is absent. Finally, in lines where deep (greater than ~200m) grabens are subducted, SU1 may be present beneath the décollement (Figures 3d and 4b), along with SU2, SU3, and SU4.

4.2 Frontal prism structure and fate of sediments

We combine our mapping of seismic units, imbricate thrust faults, and décollement position to generate criteria for identifying portions of the forearc that are the product of sediment accretion, sediment subduction, or frontal tectonic erosion (deformation "modes", Table 1). Because of the time transgressive nature of deformation during subduction, structures mapped at greater distances from the trench reflect the cumulative processes

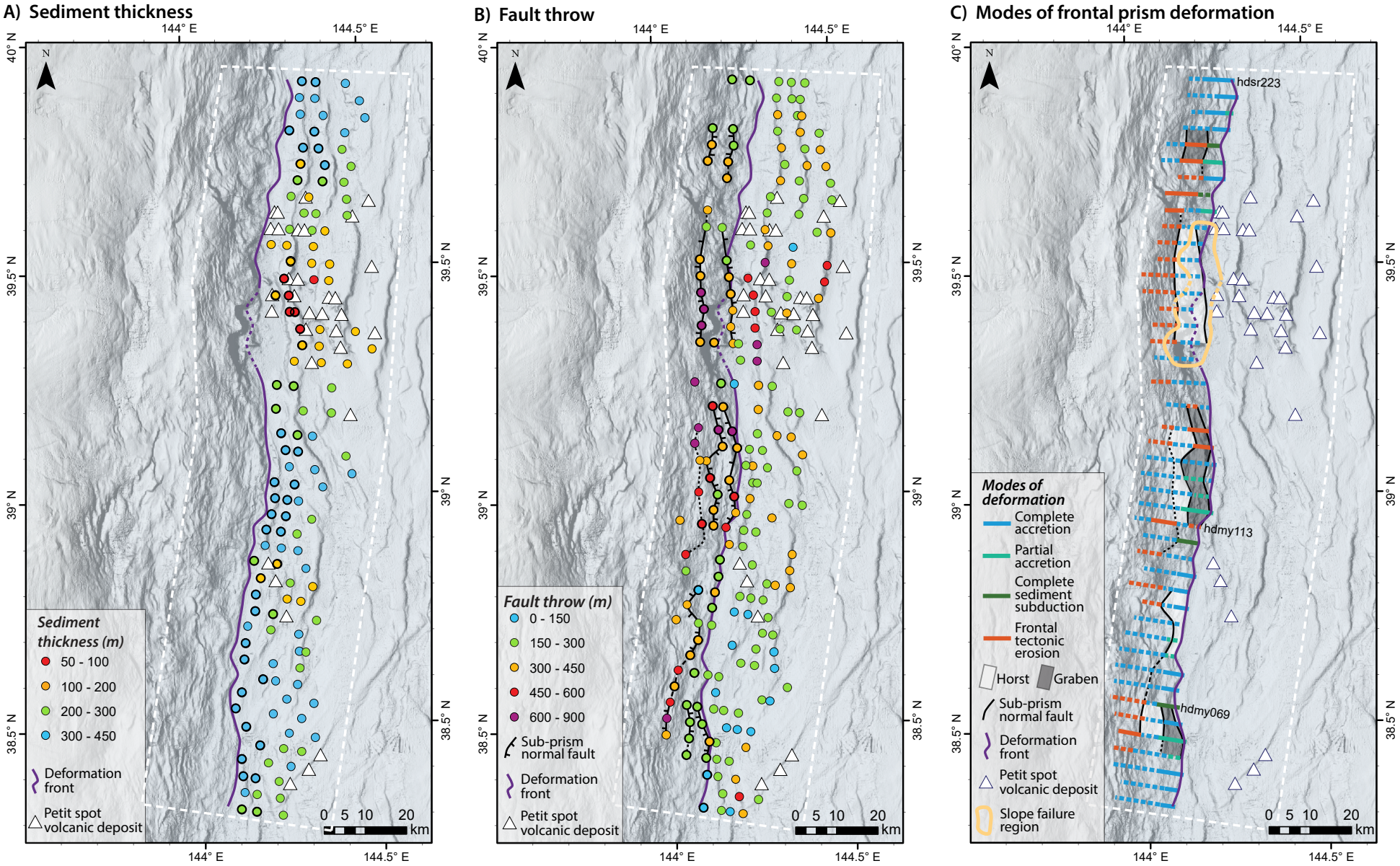

Figure 5 Caption on page 11.

that operated when that portion of the subducted plate was at the trench, while it was being translated to its current position, and those operating *in situ* today. As such, we define separate criteria to interpret each mode in the up-dip region at the deformation front, and down-dip regions ~>5km landward of the deformation front.

4.2.1 Complete sediment accretion

Near the deformation front, line segments are categorized as experiencing complete sediment accretion if they contain imbricate thrust faults in the frontal prism that sole into a décollement localized at the base of the incoming plate sediment section, SU2 (Table 1, Figure 3a). In these locations, SU3 and SU4 are located below the décollement. We interpret this geometry to indicate that the complete sediment section of SU2 is off-scraped and actively accreted to the frontal prism. Landward of the deformation front, we categorized a line segment as having experienced complete sediment accretion if the décollement separates prism sediments (SU1/SU2) in the overriding plate from the chert and basalt (SU3/4) of the subducting plate, with no incoming plate sediment (SU2) observed beneath the décollement. In these locations, we infer that the missing SU2 was previously accreted at the deformation front, and that the frontal prism is actively sliding along a décollement that is localized directly above chert/basalt of SU3/4.

4.2.2 Partial sediment accretion

Near the deformation front, line segments are categorized as experiencing partial sediment accretion if they contain thrust faults that sole into a décollement formed in a horizon within SU2 (Table 1, Figure 3b). In these locations, parallel reflections of SU2 are often observed beneath the décollement. We interpret that in these lines, the upper portion of the sediments above the décollement are actively accreting to the frontal prism and the sediments beneath the décollement are locally subducted. Landward of the deformation front, partial accretion is mapped in locations where the décollement separates prism sediments (SU1/SU2) in the overriding plate from incoming plate sediments (SU2) below the décollement. In these locations, either parallel reflectors of the lower part of SU2 are observed below the décollement, or the total thickness of SU2 under the décollement is much less than the total thickness of SU2 on the incoming plate. We infer that the missing upper section of SU2 was accreted at the deformation front, such that only the lower portion was subducted to depth. These data imply that the frontal prism is actively sliding along the décollement over the lower portion of SU2, such that there is active subduction of the lowermost incoming plate sediments.

4.2.3 Complete sediment subduction

Near the deformation front, line segments are categorized as experiencing complete sediment subduction if the décollement is localized at the top of the incoming plate sediments below prism sediments (Table 1, Figure 3c). In these locations, seismic reflectors that represent the complete thickness of the incoming plate sediments (SU2) are present beneath the décollement. Here, the complete sediment section is locally subducted and there is no active accretion occurring at the deformation front. Landward of the deformation front, complete sediment subduction is mapped using similar criteria: reflectors comprising the complete SU2 section are observed beneath the décollement. In these locations, we infer that no sediment accretion occurred at the deformation front, and that there is currently stable sliding of the prism along the décollement above the subducted sediment section.

4.2.4 Incipient frontal tectonic erosion

Frontal tectonic erosion, whereby frontal prism material is subducted to depth, has been proposed to occur by entrapment of frontal prism material under the décollement within a subducted graben (e.g., Hilde, 1983). This process has been proposed to initiate via gravitational collapse and slumping of frontal prism material that fills the incoming plate graben at the trench (e.g., Hilde, 1983; von Huene and Culotta, 1989). The slope failures and sediment slumping that we map at the trench may indicate the incipient process that can ultimately lead to frontal tectonic erosion (Figures 3d and 5c). Therefore, while we do not map frontal tectonic erosion as an active process at the deformation front, slope failures mapped at the deformation front may indicate locations where frontal tectonic erosion will occur in the future.

We can, however, map portions of line segments at depth that may be experiencing active frontal tectonic erosion. Frontal tectonic erosion is mapped at locations landward of the deformation front where a planar décollement cuts across a graben within prism sediments (SU1) such that frontal prism material and incoming plate sediments (SU2) are entrapped below the décollement within a graben (Figures 3d and 4b and c). In these locations, we infer that both tectonic erosion and subduction of incoming plate sediments is occurring. Frontal tectonic erosion is also inferred in locations where a décollement reflector is not clear, but where high relief subducted grabens are filled with SU1 and SU2. Where frontal tectonic erosion is mapped, we infer that the prism slides along the décollement and that both SU1 and SU2–4 are actively subducted.

4.3 Spatial variability in modes of deformation

Using the above criteria, we mapped modes of deformation on each seismic line, covering a region that extends ~180 km along margin strike, from the deformation front to ~20 km down dip (Figures 4 and 5c; S3–8). Our mapping shows that modes of deformation are not constant with depth along a single seismic line (Figure 5c), and only ~30% of the seismic profiles contain a single mode of deformation (e.g., Figure 4a). Most seismic lines contain two or three different deformation modes (Figures 4b and c; S4 - 8). Transitions between modes occur at horst or graben boundaries. For

Figure 5 Results of mapping seismic reflections profiles along the Japan trench. The white dashed boxes denote the extent of the seismic profiles in the study area. The purple line indicates the mapped location of the deformation front. The white triangles represent petit spot volcanic deposits on the incoming plate. **A.** Sediment thickness measurements at 130 locations on the incoming plate. **B.** Map showing measured throw along normal faults developed on the Pacific plate crust at 199 locations. Note that regions with petit spot volcanism are located with thin sediments and high offset faults. Thick outlined points in panels **A** and **B** denote sites used in ratio calculations at the trench. Only sites with both sediment thickness data within 10 km of the trench and fault throw data on the first subducted horst or graben were used. **C.** Map of modes of frontal prism deformation: solid line where certain; dashed where uncertain or inferred. These data show that prism evolution varies between sediment accretion, sediment subduction, and frontal tectonic erosion over ~5 - 10 km length scales along strike and down dip. Cross-comparisons of all three maps show that sediment accretion occurs in regions with thick incoming plate sediment and small fault throw, while slope failure and tectonic erosion tend to occur in places with thin sediments, petit spot volcanism, and large fault throw.

example, line hdmy113 (Figure 4b) is characterized by alternating modes of tectonic erosion in grabens and sediment accretion on horsts. Similarly, line hdmy069 (Figure 4c) is characterized by complete sediment subduction in a graben at the trench, complete accretion in the down-dip horst, and tectonic erosion in the next graben down dip. Our seismic line mapping shows that the mode of deformation varies in the study area over length scales of ~5–20 km along strike, and ~5–10 km down dip (Figure 5c).

Importantly, we find that the types of deformation that can occur, and therefore the possible pathways for incoming and upper plate sediments, differ between horsts and grabens. Horsts in the study area only experience complete sediment accretion or partial accretion, and do not experience tectonic erosion or sediment subduction (Figures 3, 4, and 5c; S3 - S8). This observation, apparent both at the trench and at depth, indicates that most or all of the sediment on subducted horsts is off-scraped by imbricate thrusts and accreted to the frontal prism at the deformation front.

In contrast, subducted grabens can experience any of the four modes of deformation (Figure 5c). Our mapping shows approximately half of the grabens experience complete or partial accretion and half experience complete sediment subduction or tectonic erosion. This observation of sediment accretion in grabens directly contrasts prior models that suggest subducted grabens ubiquitously lead to sediment subduction and promote frontal tectonic erosion (e.g., Hilde, 1983; von Huene and Culotta, 1989). Instead, our data imply that other processes may control whether sediments in a subducted graben will be accreted, subducted, or tectonically eroded.

4.4 Correlations between sediment thickness, fault throw, and frontal prism deformation

The relative magnitudes of outer-rise fault throw and incoming plate sediment thickness at the time of subduction may play a key role in sediment flux and prism evolution. We test this hypothesis by correlating the maps of frontal prism deformation mode with measurements of fault offset and sediment thickness on the incoming plate at the trench (Figure 6). Along each seismic line, we calculate the weighted-average fault throw from the first one to two normal faults subducted beneath the frontal prism and average sediment thickness using measurements within ~10km of the trench (See Figure 4 for measurement locations). We then correlate these near-trench values with the mode of deformation mapped closest to the trench in order to determine variations in sediment thickness and fault throw as a function of deformation mode.

We find that incoming plate sediment thicknesses are similar (~300–365 m) in regions experiencing complete accretion, partial accretion, complete sediment subduction, and frontal tectonic erosion, whereas sediment thickness outboard of regions with slope failures are exceptionally low (115 ± 45 m) (Figure 6a). We find that fault throw varies between the different modes of deformation, where larger fault throw values correlate to smaller volumes of accreted sediment. Complete sediment accretion occurs where the subducting oceanic crust has the smallest average fault throws of 216 ± 65 m. Partial accretion and complete sediment subduction occur where the subducting crust has intermediate fault throws of ~295–340 m (Figure 6b). Portions of the margin experiencing frontal tectonic erosion and slope failure have significantly larger fault throws, averaging around ~490 - 500 m.

We evaluate this relationship between the incoming plate and frontal prism deformation by combining sediment thickness and fault throw measurements (Figure 6a-b) into a single ratio using near-trench measurements and correlate these near-trench ratios to the mode of deformation mapped closest to the trench (Figure 6c). These ratio data show discrete variations between the relative magnitudes of sediment thickness and fault throw as a function of deformation mode. Complete sediment accretion occurs inboard of regions where there is a high ratio of sediment thickness to fault throw (1.50 ± 0.6) (Figure 6c). Partial sediment accretion and complete sediment subduction occur inboard of regions where the ratio of sediment thickness to fault throw on the incoming plate have intermediate values of 1.09 ± 0.2 and 1.25 ± 0.2 respectively. Frontal tectonic erosion occurs inboard of regions with a low ratio of sediment thickness to fault throw (0.72 ± 0.2). Lastly, slope failures at the deformation front occur where the lowest ratio of sediment thickness to fault throw (0.28 ± 0.2).

We note that the total number of observations for some modes of deformation is small (n=2 to 6). If we

Mode of deformation	At deformation front		Landward of deformation front	
	Mapping criteria (observations)	Interpreted processes	Mapping criteria (observations)	Interpreted processes
Complete sediment accretion	• Imbricate thrust faults sole into the décollement • Décollement is localized at the base of the incoming plate sediment section (SU2) • SU3 and SU4 are below the décollement	• Complete incoming sediment section is actively accreting to the frontal prism	• Décollement is localized above chert/basalt (SU3/SU4) • No incoming plate sediment (SU2) is observed beneath the décollement	• Prism (SU1) is sliding along décollement • Incoming plate sediment (SU2) was previously accreted
Partial sediment accretion	• Imbricate thrust faults sole into the décollement • Décollement is localized within the incoming plate sediment section (SU2) • Parallel reflections of lower SU2 are present beneath décollement	• Upper portion of incoming plate sediments (SU2) is actively accreting • Lower portion of SU2 is locally subducted	• Décollement separates prism sediments (SU1/SU2) from lower portion of incoming plate sediments (SU2) • Parallel reflectors of SU2 observed below décollement	• Prism (SU1) is sliding along décollement • Upper portion of SU2 was previously accreted • Lower portion of SU2 is locally subducted
Complete sediment subduction	• Décollement is localized between the prism sediments (SU1) and the top of the incoming plate sediments (SU2) • Complete set of SU2 reflections is present beneath the décollement	• Complete sediment section is locally subducted; no accretion occurring	• Décollement is localized at the top of the incoming plate sediment section (SU2) • Parallel reflectors (SU2) are present beneath décollement • Décollement separates prism sediments (SU1) and incoming plate sediments (SU2)	• Prism (SU1) is sliding on top of subducted sediment section (SU2) • Sediments below décollement are being subducted • No accretion has occurred
Slope failures and incipient frontal tectonic erosion	• *Frontal tectonic erosion does not occur at the deformation front; it only occurs landward of the deformation front*	• *The precursor to frontal tectonic erosion may be slope failures at the deformation front and mass transport deposits into a subducting graben*	• Planar décollement cuts across a graben within prism sediments (SU1), connecting two adjacent horsts • Frontal prism material (SU1) and incoming plate sediments (SU2) are entrapped below the décollement within a graben	• Stable sliding across décollement • Frontal prism sediments (SU1) and incoming plate sediments (SU2) within graben are locally subducted

Table 1 Criteria for mapping modes of frontal prism deformation.

increase the number of observations by correlating all measurements of fault throw and sediment thickness on the incoming and subducted plates with each type of deformation mode at the trench, we see similar relative relationships between fault throw, sediment thickness, and deformation mode. However, these data show greater overlap, with ratios of 1.15 ± 0.6 for sediment accretion, 1.15 ± 0.4 for partial accretion, 1.06 ± 0.4 for complete sediment subduction, 0.94 ± 0.5 for frontal tectonic erosion, and 0.41 ± 0.2 m for slope failure (Figure S9). Similarity in these values may be the result of averaging across variable fault throws and sediment thicknesses that exist over larger areas (~15–20 km) as compared to near trench data (5–10 km) (Figures 5 and 6d). This suggests near-trench values of sediment thickness and fault throw are the better predictor of deformation mode at the trench. These data also suggest that small-spatial scale variation in fault throw or sediment thickness on the incoming plate can lead to significant spatio-temporal variation in deformation mode at the

trench.

5 Discussion

5.1 Influence of sediment thickness and fault throw on modes of frontal prism deformation and sediment flux

Modes of frontal prism deformation and the fate of both incoming and upper plate sediments are a direct function of whether horsts or grabens are being subducted and the relative magnitudes of fault offset versus sediment thickness. First, we find that sediment accretion always occurs on horsts, but grabens experience all modes of deformation. Second, we find that sediment accretion at the deformation front is promoted where there are thicker incoming plate sediments (~300 m) and outer-rise faults with low offsets (~225 m); that is, in regions where the ratio of sediment thickness to fault throw is >1 (Figures 5 and 6). Third, we find that locations on the incoming plate where there is petit spot volcanism, moderate or thin sediments (<~300 m), and outer-rise faults with large offsets (>350 m) correlate to locations on the overriding plate with slope failures and frontal tectonic erosion, where the ratio is <1 (Figures 5 and 6). These observations suggest that there may be a critical threshold of sediment thickness to fault throw that controls the modes of deformation and sediment flux in the presence of subducting grabens. At the Japan trench, this threshold appears to be approximately 1:1 ratio of sediment thickness to normal fault throw.

5.2 Implications for décollement heterogeneity

Spatio-temporal variations in the ratios of incoming plate sediment thickness to outer-rise fault throw, and thus modes of frontal prism deformation, directly impact décollement geometry and mechanics by dictating the stratigraphic position of the décollement and by introducing geometric barriers (horsts and grabens) to the décollement. We observe spatial variations over short length-scales (~5–10 km) in both frontal prism mode of deformation and incoming plate ratio of sediment thickness to fault throw (Figures 5 and 6d). Therefore, equivalent heterogeneity in décollement geometry and composition must occur at similar spatial scales.

Our data suggest that there may be a threshold of fault throw, given an incoming sediment thickness, that if exceeded, disrupts the décollement's ability to localize at the base of the incoming sediment section. For normal fault throws below this threshold (ratio >1), a single continuous, undulating décollement can develop that promotes sediment accretion (Figure 7a). For fault throws above this threshold (ratio <1), a planar décollement develops across a graben that is mechanically more favorable to propagate that promotes sediment subduction and frontal tectonic erosion (Figure 7b).

Variations in the occurrence of sediment accretion, sediment subduction, and frontal tectonic erosion therefore have direct implications for two types of heterogeneity on the shallow décollement: geometric heterogeneity and compositional heterogeneity. First, subducting horsts and grabens on the incoming plate modulate shallow décollement mechanics by creating geometric barriers over which the décollement must propagate. We observe two different endmember geometries of the décollement where it interacts with horst and graben topography. At the Japan trench, when sediment thickness is large relative to fault throw, we observe that the décollement undulates with subducting topography, stepping up and down subducted normal faults to maintain its position in a similar stratigraphic horizon (e.g., Figures 4a and 7a). This stepping, however, creates geometric barriers over which the prism must slide, and these barriers may create local stress heterogeneities along the shallow megathrust (e.g., Sun et al., 2020). In contrast, when sediment thickness is small relative to fault throw, we observe that the décollement does not step down into the graben, but instead attempts to maintain its planarity as it propagates across the adjacent graben (e.g., Figures 4b and 7b). This planar décollement "smooths" over the subducting topographic roughness generated by normal faults without developing normal fault-related geometric barriers in the shallow megathrust. Therefore, the ratio of sediment thickness to fault offset on the incoming plate may be used to infer the degree of geometric heterogeneity present in the shallow décollement, where high ratios predict undulating décollements that step over geometric barriers, and low ratios predict planar décollements that smooth over these barriers.

Second, spatial heterogeneity in the mode of frontal prism deformation requires correlative heterogeneity in the composition of the shallow décollement. This is because in systems with subducting outer-rise normal faults, the juxtaposition of upthrown and downthrown horst and graben blocks on the incoming plate creates lateral variations in the incoming plate sediment section. A décollement that has a planar geometry that cuts across subducting grabens will inherently propagate across different sedimentary units. In contrast, a décollement that undulates with the subducting topography may remain in a continuous stratigraphic horizon. In the Japan trench, where sediment thickness is large relative to fault throw, we observe that the décollement undulates with subducting horsts and graben topography in order to remain in the same stratigraphic position near the SU3 - SU2 contact (Figure 7a). Conversely, where sediment thickness is small relative to fault throw, the décollement is planar and may cut across different lithologic units, including SU2 and SU1, introducing compositional heterogeneity to the décollement (Figure 7b). Therefore, the ratio of sediment thickness to fault throw on the subducting plate may be a predictor for compositional heterogeneity on the shallow plate interface, where high ratios correlate to compositionally homogenous décollement segments and low ratios correlate to heterogeneous décollement segments.

These observations imply that, in portions of the Japan trench where sediment thickness is greater than normal fault throw, it is mechanically more favorable for the décollement to make a small bend and remain in a continuous stratigraphic horizon than to develop a new décollement segment that smooths over subduct-

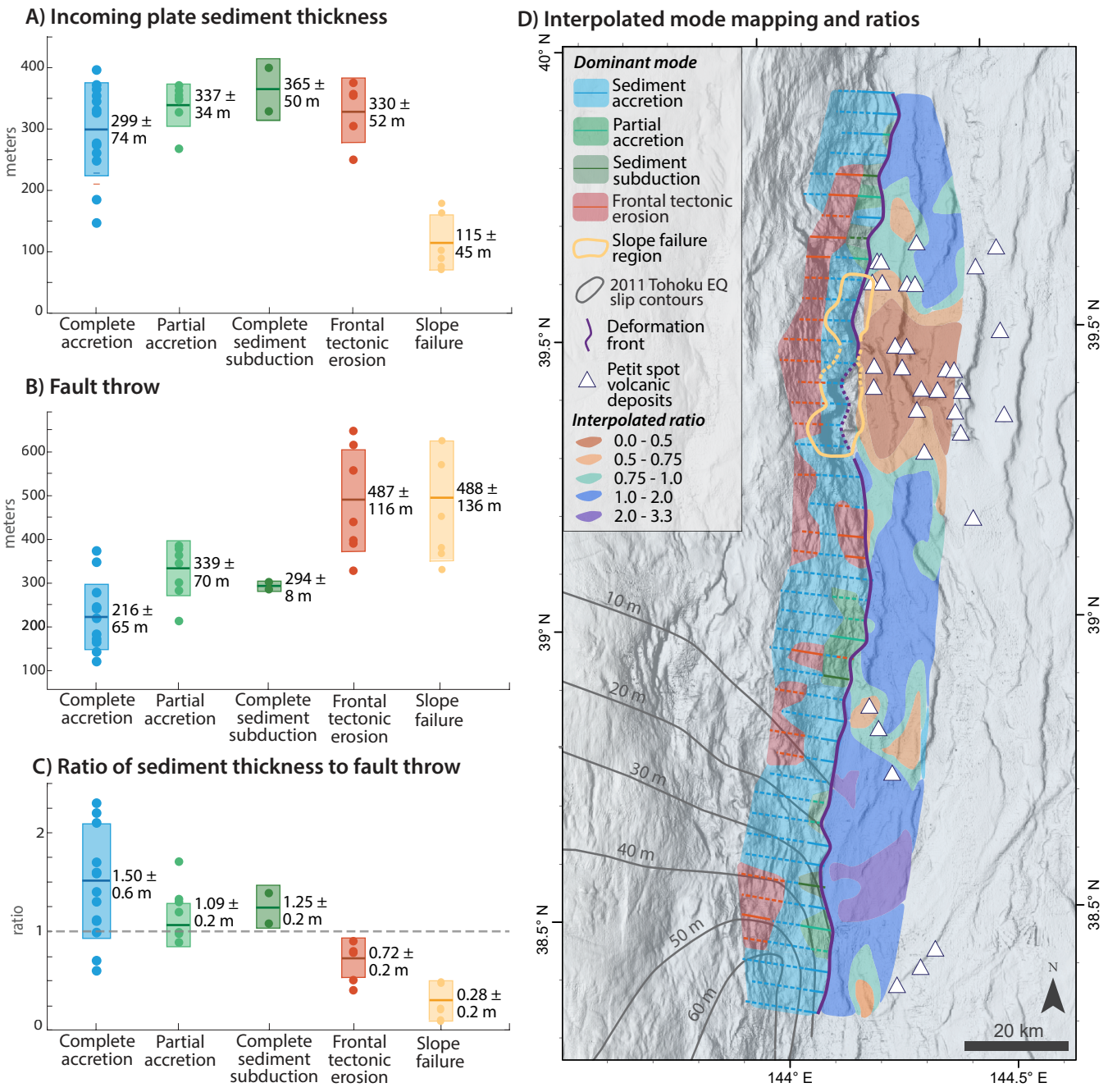

Figure 6 Comparisons between sediment thickness, fault throw, and mode of frontal prism deformation at the trench. Box plots **(A - C)** include individual measurements (points), weighted averages (horizontal line), and $2\sigma_w$ uncertainty (boxes). See Figure 4 for measurement locations. **A.** Sediment thickness as a function deformation mode. Average sediment thickness is the smallest outboard of regions with slope failures. Average sediment thickness is similar in regions experiencing all other modes. **B.** Fault throw as a function of deformation mode. Portions of the prism experiencing complete accretion have the smallest average fault throw, followed by partial accretion and full sediment subduction, frontal tectonic erosion, and regions with slope failures. **C**. Ratio of sediment thickness to fault throw as a function of deformation mode. Regions experiencing complete accretion, partial accretion, and complete sediment subduction have ratios >1. Regions experiencing tectonic erosion or slope failure have ratios <1. **D.** Map of dominant prism deformation mode, interpolated sediment thickness to fault throw ratio on the incoming plate (1km grid), and slip contours for the 2011 Tohoku earthquake (after Iinuma et al., 2012).

ing topography. Only when normal fault throw is large is it more favorable to develop a new planar décollement segment that propagates through subducting sediments or frontal prism. This mechanical favorability may be influenced, at least in part, by the frictional properties of the sediments in the incoming section. Coring of the incoming plate, frontal prism, and décollement at IODP site C0019 and DSDP site 436 show that the décollement is locally developed within the basal, smectite rich clay layer, correlative to the basal portion of SU2 on the incoming plate (Chester et al., 2013; Nakamura et al., 2013; Kirkpatrick et al., 2015; Nasu et al., 1980). Friction experiments indicate that these basal clays have high concentrations of smectite and lower friction co-

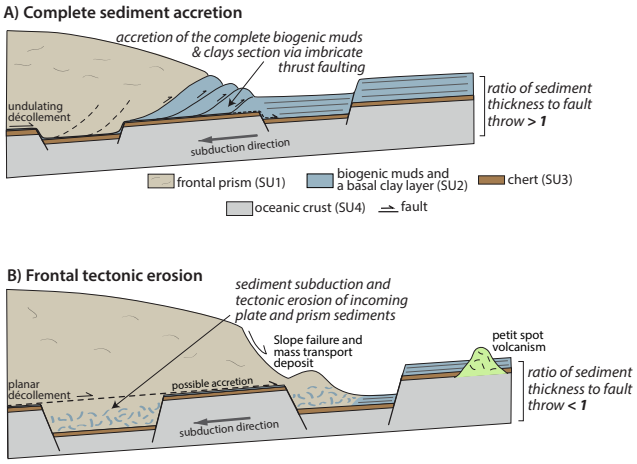

Figure 7 Endmember models of modes of frontal prism deformation based on a synthesis of mapped seismic reflection lines in survey KR13-11 along the Japan trench. **A.** Sediment accretion is promoted in regions where sediment thickness on the incoming plate is large relative to incoming plate fault throw on outer-rise faults (ratio >1). In this scenario, the décollement undulates with subducting horsts and grabens and may remain in the basal clay layer. **B.** Frontal tectonic erosion is promoted in regions with small sediment thickness relative to fault throw (ratio <1). At the Japan trench, the presence of petit spot volcanism may contribute slope failures at the deformation front and facilitate frontal tectonic erosion.

efficients than the overlying biogenic mudstones (Ikari et al., 2015). Correlation of cores to seismic reflection lines imply that this clay layer is present across the study area, near the base of seismic unit SU2 (Nakamura et al., 2013) (Figure 1, Core C0019), except in regions where there is petit spot volcanism (Fujie et al., 2020). Therefore, the presence of this frictionally weak clay may help promote the development of undulating décollements that step into grabens in regions of low fault throw, but segmentation of the clay layer may hinder this process, leading to a planar décollement and compositional décollement heterogeneity.

Our data therefore provide important insights into the spatial scales of décollement heterogeneity that occur in the shallow subduction interface. Our frontal prism mapping suggests that relatively compositionally homogenous patches of décollement hosted in frictionally weak clays may occur in 5–20 km wide by 15–40 km long regions experiencing sediment accretion (Figure 6d). These homogeneous regions are likely segmented by ~5 km wide by 5–30 km long patches, or potential asperities, where the décollement is hosted in frictionally stronger biogenic muds and frontal prism material, in locations where partial accretion, sediment subduction, and tectonic erosion are mapped (Figure 6d).

Similar patterns can be observed in the interpolated map of incoming plate ratios (Figure 6d). This map shows 5–20 km wide by 20 to >40 km long laterally continuous regions of crust with ratios >1 that will likely promote sediment accretion and the formation of compositionally homogenous décollement patches. These patches are segmented by regions with ratios <1, where deformation mode, and therefore décollement mechanics, will likely vary over ~5–10 km length scales. These length scales are similar to those observed on the interpolated map of frontal prism deformation mode (Figure 6d). The incoming plate ratio map, therefore, may serve as a tool for interpreting patterns and length scales of spatio-temporal heterogeneity on the shallow plate interface caused by variations in décollement geometry and composition.

5.3 Implications for slip potential

The compositional and frictional properties of the décollement in northeast Japan have been proposed to be important factors in accommodating shallow seismogenic slip to the trench (e.g., Chester et al., 2013; Kameda et al., 2015; Moore et al., 2015). In particular, structural and lithological descriptions of cores and borehole logs crossing the plate boundary (Chester et al., 2013), interpretations of high-resolution seismic reflection data across the trench (Nakamura et al., 2013), and frictional heating across the plate boundary (Fulton et al., 2013) suggest that the Tohoku earthquake slip surface localized in the basal zone of frictionally weak, smectite-rich pelagic clay. Additionally, published seismic reflection data collected across the portion of the earthquake with the greatest amount of slip show a deformation front with imbricate thrust faults that sole into the décollement, positioned near the base of the sediment section, that undulates with subducting horsts and grabens (Boston et al., 2014; Chester and Moore, 2018; Nakamura et al., 2013, 2020). The décollement and the branching imbricate thrust faults have been suggested to be the shallowest faults that hosted Tohoku earthquake slip (Nakamura et al., 2020).

The degree of heterogeneity along the plate interface imparted by outer-rise normal fault subduction may influence seismogenic slip to the trench. Specifically, we find that in the southern portion of the map area (south of 39°N) where shallow slip occurred during the 2011 Tohoku earthquake, incoming plate sediment thickness is mainly greater than fault throw (ratio >1) and complete or partial sediment accretion are the predominant modes of deformation. These data suggest that the upper ~20 km of the shallow subduction interface in this region may have a relatively lithologically homogenous and frictionally weak composition that promotes shallow seismogenic slip. These interpretations agree with prior work which demonstrates that the region of large slip during the Tohoku earthquake occurred in regions experiencing sediment accretion via imbricate thrust faulting (Nakamura et al., 2020).

Conversely, in the northern portion of the map area (~39.1–39.7°N), there is greater variability in the mapped deformation modes and lower ratios of sediment thickness to fault throw at the trench. These data suggest the décollement here may be compositionally heterogeneous and may be developed in frictionally stronger materials. This portion of the margin is known to host tectonic tremors and transient aseismic slip (e.g., Nishikawa et al., 2023). We identify two pos-

sible sources of heterogeneity in the shallow plate interface in this region. First, the incoming plate outboard of this region contains thin sediments and petit spot volcanism (Figure 5). Petit spot volcanism is thought to thermally metamorphose the incoming plate sediment section, which alters the compositional properties and may increase the friction of these biogenic muds and clays (Fujie et al., 2020). Therefore, in these locations, the compositional and frictional properties of the incoming plate sediments are different than the surrounding, unaltered incoming plate sediments, and may disrupt décollement development and limit slip potential in these areas. Second, this region contains large-offset normal faults on the incoming plate (ratios <1) that may also disrupt décollement development by introducing large geometric asperities and by promoting lateral heterogeneity in the composition and frictional properties of the sediments in which the décollement develops. Such geometric asperities and lateral variations in compositional and frictional properties of the décollement have been thought to inhibit large magnitude slip to the trench (Kodaira et al., 2019; Fujie et al., 2020; Moore et al., 2015; Qin et al., 2022). Therefore, our results demonstrate that sediment thickness and outer-rise fault throw may exert a significant control on the composition, friction, and geometric heterogeneity of the décollement that may help promote or inhibit large magnitude, shallow tsunamigenic slip. These relationships have important implications for slip potential at the Japan trench as well as in sediment-starved subduction systems globally where outer-rise normal faults are subducted.

6 Conclusion

Outer-rise faults and sediment thickness on the incoming plate are direct inputs into the shallow subduction zone, and therefore have an important influence on frontal prism modes of deformation, décollement evolution, and the potential for shallow plate boundary slip. We mapped sediment thickness on the incoming plate, the amount of fault throw across normal faults that bound horsts and grabens, instances of petit spot volcanism on the incoming plate, and slope failures at the deformation front for a portion of the Japan trench. We show heterogeneity in the modes of frontal prism deformation at 5–10 km length scales along strike and down dip. We find that portions of the incoming plate where sediment thickness is greater than fault throw may promote sediment accretion and the development of an undulating, lithologically homogenous décollement. Conversely, subduction of incoming plate segments with a thin sediment section and high offset faults may promote tectonic erosion and slope failures, and the development of a planar but lithologically heterogeneous décollement that smooths over subducting horsts and grabens.

The degree of heterogeneity observed in the frontal prism deformation mode requires correlative geometric and compositional heterogeneity in the shallow décollement and may have important implications for the mechanics of and potential for shallow plate boundary slip. In particular, the 2011 Tohoku earthquake ruptured the southern portion of the study area, where outer-rise fault throws are small relative to sediment thickness and sediment accretion is the dominant mode of deformation and ended in a region that transitions to high fault throw and thin sediments. Because the Japan trench has a range of sediment thicknesses and fault throws that are characteristic to many sediment-starved margins around the globe, we propose that the ratio of sediment thickness to fault throw may be a useful proxy for understanding how outer-rise fault throw and incoming sediment thickness impact frontal prism deformation style, sediment flux, and décollement heterogeneity at other margins.

Acknowledgements

Funding for this project was provided by the National Science Foundation grant OCE-2103514 and the Northern Arizona University Duebendorfer & Barnes Structural Geology Endowment and Eminent Scholars Foundations. Data collection and processing were supported by the Japan Agency for Marine-Earth Science and Technology (JASMTEC). We thank IHS S&P Global for providing academic licenses for their Kingdom Suite software. We also thank Rebecca Bell and Harold Tobin for their constructive reviews that helped improve this manuscript.

7 Data and code availability

The seismic reflections profiles used in this study can be requested and accessed from https://www.jamstec.go.jp/obsmcs_db/e/. Data tables in this study can be found in the Supporting Information and on Zenodo (Schottenfels et al., 2023).

8 Competing interests

The authors have no competing interests.

References

Boston, B., Moore, G. F., Nakamura, Y., and Kodaira, S. Outer-rise normal fault development and influence on near-trench décollement propagation along the Japan Trench, off Tohoku. *Earth, Planets and Space*, 66(1):135, 2014. doi: 10.1186/1880-5981-66-135.

Chester, F. M. and Moore, J. C. *Tectonostratigraphy and processes of frontal accretion with horst-graben subduction at the Japan Trench*. Geological Society of America, 2018. doi: 10.1130/2018.2534(06).

Chester, F. M., Rowe, C., Ujiie, K., Kirkpatrick, J., Regalla, C., Remitti, F., Moore, J. C., Toy, V., Wolfson-Schwehr, M., Bose, S., Kameda, J., Mori, J. J., Brodsky, E. E., Eguchi, N., and Toczko, S. Structure and Composition of the Plate-Boundary Slip Zone for the 2011 Tohoku-Oki Earthquake. *Science*, 342(6163):1208–1211, Dec. 2013. doi: 10.1126/science.1243719.

Clift, P. and Vannucchi, P. Controls on tectonic accretion versus erosion in subduction zones: Implications for the origin and recycling of the continental crust. *Reviews of Geophysics*, 42(2), Apr. 2004. doi: 10.1029/2003rg000127.

Contreras-Reyes, E., Grevemeyer, I., Flueh, E. R., Scherwath, M., and Heesemann, M. Alteration of the subducting oceanic lithosphere at the southern central Chile trench–outer rise. *Geochemistry, Geophysics, Geosystems*, 8(7), July 2007. doi: 10.1029/2007gc001632.

Fujie, G., Kodaira, S., Nakamura, Y., Morgan, J. P., Dannowski, A., Thorwart, M., Grevemeyer, I., and Miura, S. Spatial variations of incoming sediments at the northeastern Japan arc and their implications for megathrust earthquakes. *Geology*, 48(6):614–619, Mar. 2020. doi: 10.1130/g46757.1.

Fujiwara, T., Hirano, N., Abe, N., and Takizawa, K. Subsurface structure of the "petit-spot" volcanoes on the northwestern Pacific Plate. *Geophysical Research Letters*, 34(13), July 2007. doi: 10.1029/2007gl030439.

Fulton, P. M., Brodsky, E. E., Kano, Y., Mori, J., Chester, F., Ishikawa, T., Harris, R. N., Lin, W., Eguchi, N., and Toczko, S. Low Coseismic Friction on the Tohoku-Oki Fault Determined from Temperature Measurements. *Science*, 342(6163):1214–1217, Dec. 2013. doi: 10.1126/science.1243641.

Hilde, T. W. Sediment subduction versus accretion around the pacific. *Tectonophysics*, 99(2–4):381–397, Dec. 1983. doi: 10.1016/0040-1951(83)90114-2.

Hirano, N., Takahashi, E., Yamamoto, J., Abe, N., Ingle, S. P., Kaneoka, I., Hirata, T., Kimura, J.-I., Ishii, T., Ogawa, Y., Machida, S., and Suyehiro, K. Volcanism in Response to Plate Flexure. *Science*, 313(5792):1426–1428, Sept. 2006. doi: 10.1126/science.1128235.

Hirano, N., Machida, S., Sumino, H., Shimizu, K., Tamura, A., Morishita, T., Iwano, H., Sakata, S., Ishii, T., Arai, S., Yoneda, S., Danhara, T., and Hirata, T. Petit-spot volcanoes on the oldest portion of the Pacific plate. *Deep Sea Research Part I: Oceanographic Research Papers*, 154:103142, Dec. 2019. doi: 10.1016/j.dsr.2019.103142.

Iinuma, T., Hino, R., Kido, M., Inazu, D., Osada, Y., Ito, Y., Ohzono, M., Tsushima, H., Suzuki, S., Fujimoto, H., and Miura, S. Coseismic slip distribution of the 2011 off the Pacific Coast of Tohoku Earthquake (M9.0) refined by means of seafloor geodetic data. *Journal of Geophysical Research: Solid Earth*, 117(B7), July 2012. doi: 10.1029/2012jb009186.

Ikari, M. J., Kameda, J., Saffer, D. M., and Kopf, A. J. Strength characteristics of Japan Trench borehole samples in the high-slip region of the 2011 Tohoku-Oki earthquake. *Earth and Planetary Science Letters*, 412:35–41, Feb. 2015. doi: 10.1016/j.epsl.2014.12.014.

Ikehara, K., Usami, K., Kanamatsu, T., Arai, K., Yamaguchi, A., and Fukuchi, R. Spatial variability in sediment lithology and sedimentary processes along the Japan Trench: use of deep-sea turbidite records to reconstruct past large earthquakes. *Geological Society, London, Special Publications*, 456(1):75–89, Mar. 2017. doi: 10.1144/sp456.9.

Kameda, J., Shimizu, M., Ujiie, K., Hirose, T., Ikari, M., Mori, J., Oohashi, K., and Kimura, G. Pelagic smectite as an important factor in tsunamigenic slip along the Japan Trench. *Geology*, 43 (2):155–158, Feb. 2015. doi: 10.1130/g35948.1.

Kirkpatrick, J. D., Rowe, C. D., Ujiie, K., Moore, J. C., Regalla, C., Remitti, F., Toy, V., Wolfson-Schwehr, M., Kameda, J., Bose, S., and Chester, F. M. Structure and lithology of the Japan Trench subduction plate boundary fault. *Tectonics*, 34(1):53–69, Jan. 2015. doi: 10.1002/2014tc003695.

Kodaira, S., No, T., Nakamura, Y., Fujiwara, T., Kaiho, Y., Miura, S., Takahashi, N., Kaneda, Y., and Taira, A. Coseismic fault rupture at the trench axis during the 2011 Tohoku-oki earthquake. *Nature Geoscience*, 5(9):646–650, Aug. 2012. doi: 10.1038/ngeo1547.

Kodaira, S., Nakamura, Y., Yamamoto, Y., Obana, K., Fujie, G., No, T., Kaiho, Y., Sato, T., and Miura, S. Depth-varying structural characters in the rupture zone of the 2011 Tohoku-oki earthquake. *Geosphere*, 13(5):1408–1424, Sept. 2017. doi: 10.1130/ges01489.1.

Kodaira, S., Nakamura, Y., Fujie, G., and Miura, S. Marine active-source seismic studies in the Japan Trench: a seismogenic zone in an ocean-continent collision zone. *Acta Geologica Sinica - English Edition*, 93(S1):94–95, May 2019. doi: 10.1111/1755-6724.13959.

Kodaira, S., Fujiwara, T., Fujie, G., Nakamura, Y., and Kanamatsu, T. Large Coseismic Slip to the Trench During the 2011 Tohoku-Oki Earthquake. *Annual Review of Earth and Planetary Sciences*, 48(1):321–343, May 2020. doi: 10.1146/annurev-earth-071719-055216.

Masson, D. G. Fault patterns at outer trench walls. *Marine Geophysical Researches*, 13(3):209–225, Aug. 1991. doi: 10.1007/bf00369150.

Moore, G. F., Shipley, T. H., and Lonsdale, P. F. Subduction erosion versus sediment offscraping at the toe of the Middle America Trench off Guatemala. *Tectonics*, 5(4):513–523, Aug. 1986. doi: 10.1029/tc005i004p00513.

Moore, J. C., Plank, T. A., Chester, F. M., Polissar, P. J., and Savage, H. M. Sediment provenance and controls on slip propagation: Lessons learned from the 2011 Tohoku and other great earthquakes of the subducting northwest Pacific plate. *Geosphere*, 11(3):533–541, Apr. 2015. doi: 10.1130/ges01099.1.

Morgan, J. K., Ramsey, E. B., and Ask, M. V. S. *8. Deformation and Mechanical Strength of Sediments at the Nankai Subduction Zone: Implications for Prism Evolution and Décollement Initiation and Propagation*, page 210–256. Columbia University Press, Dec. 2007. doi: 10.7312/dixo13866-008.

Nakamura, Y., Kodaira, S., Miura, S., Regalla, C., and Takahashi, N. High-resolution seismic imaging in the Japan Trench axis area off Miyagi, northeastern Japan. *Geophysical Research Letters*, 40 (9):1713–1718, May 2013. doi: 10.1002/grl.50364.

Nakamura, Y., Fujiwara, T., Kodaira, S., Miura, S., and Obana, K. Correlation of frontal prism structures and slope failures near the trench axis with shallow megathrust slip at the Japan Trench. *Scientific Reports*, 10(1), July 2020. doi: 10.1038/s41598-020-68449-6.

Nakamura, Y., Kodaira, S., Fujie, G., Yamashita, M., Obana, K., and Miura, S. Incoming plate structure at the Japan Trench subduction zone revealed in densely spaced reflection seismic profiles. *Progress in Earth and Planetary Science*, 10(1), Aug. 2023. doi: 10.1186/s40645-023-00579-7.

Nasu, N., von Huene, R., Ishiwada, Y., Langseth, L., Bruns, T., and Honza, E. *Interpretation of Multichannel Seismic Reflection Data, Legs 56 and 57, Japan Trench Transect, Deep Sea Drilling Project*. U.S. Government Printing Office, Nov. 1980. doi: 10.2973/dsdp.proc.5657.112.1980.

Nishikawa, T., Ide, S., and Nishimura, T. A review on slow earthquakes in the Japan Trench. *Progress in Earth and Planetary Science*, 10(1), Jan. 2023. doi: 10.1186/s40645-022-00528-w.

Polet, J. and Kanamori, H. Shallow subduction zone earthquakes and their tsunamigenic potential. *Geophysical Journal International*, 142(3):684–702, Sept. 2000. doi: 10.1046/j.1365-246x.2000.00205.x.

Qin, Y., Nakamura, Y., Kodaira, S., and Fujie, G. Seismic imaging of subsurface structural variations along the Japan trench south of the 2011 Tohoku earthquake rupture zone. *Earth and Planetary Science Letters*, 594:117707, Sept. 2022. doi: 10.1016/j.epsl.2022.117707.

Regalla, C., Bierman, P., and Rood, D. H. Meteoric 10Be Reveals a

Young, Active Accretionary Prism and Structurally Complex Décollement in the Vicinity of the 2011 Tohoku Earthquake Rupture. *Geochemistry, Geophysics, Geosystems*, 20(11):4956–4971, Nov. 2019. doi: 10.1029/2019gc008483.

Saffer, D. M. and Tobin, H. J. Hydrogeology and Mechanics of Subduction Zone Forearcs: Fluid Flow and Pore Pressure. *Annual Review of Earth and Planetary Sciences*, 39(1):157–186, May 2011. doi: 10.1146/annurev-earth-040610-133408.

Sawai, M., Niemeijer, A. R., Hirose, T., and Spiers, C. J. Frictional properties of JFAST core samples and implications for slow earthquakes at the Tohoku subduction zone. *Geophysical Research Letters*, 44(17):8822–8831, Sept. 2017. doi: 10.1002/2017gl073460.

Schottenfels, E., Regalla, C., and Nakamura, Y. Influence of outer-rise faults on sediment flux and décollement heterogeneity at the Japan trench, 2023. doi: 10.5281/zenodo.7683455.

Seno, T., Stein, S., and Gripp, A. E. A model for the motion of the Philippine Sea Plate consistent with NUVEL-1 and geological data. *Journal of Geophysical Research: Solid Earth*, 98(B10): 17941–17948, Oct. 1993. doi: 10.1029/93jb00782.

Shipboard Scientific Party. *Site 436, Japan Trench Outer Rise, Leg 56*. U.S. Government Printing Office, Nov. 1980. doi: 10.2973/dsdp.proc.5657.107.1980.

Strasser, M., Kölling, M., Ferreira, C. d. S., Fink, H., Fujiwara, T., Henkel, S., Ikehara, K., Kanamatsu, T., Kawamura, K., Kodaira, S., Römer, M., and Wefer, G. A slump in the trench: Tracking the impact of the 2011 Tohoku-Oki earthquake. *Geology*, 41(8): 935–938, Aug. 2013. doi: 10.1130/g34477.1.

Sun, T., Saffer, D., and Ellis, S. Mechanical and hydrological effects of seamount subduction on megathrust stress and slip. *Nature Geoscience*, 13(3):249–255, Mar. 2020. doi: 10.1038/s41561-020-0542-0.

Tanioka, Y., Ruff, L., and Satake, K. What controls the lateral variation of large earthquake occurrence along the Japan Trench? *Island Arc*, 6(3):261–266, Sept. 1997. doi: 10.1111/j.1440-1738.1997.tb00176.x.

Tsuru, T., Park, J., Takahashi, N., Kodaira, S., Kido, Y., Kaneda, Y., and Kono, Y. Tectonic features of the Japan Trench convergent margin off Sanriku, northeastern Japan, revealed by multichannel seismic reflection data. *Journal of Geophysical Research: Solid Earth*, 105(B7):16403–16413, July 2000. doi: 10.1029/2000jb900132.

Tsuru, T., Park, J., Miura, S., Kodaira, S., Kido, Y., and Hayashi, T. Along-arc structural variation of the plate boundary at the Japan Trench margin: Implication of interplate coupling. *Journal of Geophysical Research: Solid Earth*, 107(B12), Dec. 2002. doi: 10.1029/2001jb001664.

von Huene, R. and Culotta, R. Tectonic erosion at the front of the Japan Trench convergent margin. *Tectonophysics*, 160(1–4): 75–90, Mar. 1989. doi: 10.1016/0040-1951(89)90385-5.

von Huene, R. and Lallemand, S. Tectonic erosion along the Japan and Peru convergent margins. *Geological Society of America Bulletin*, 102(6):704–720, June 1990. doi: 10.1130/0016-7606(1990)102<0704:teatja>2.3.co;2.

von Huene, R., Langseth, M., Nasu, N., and Okada, H. A summary of Cenozoic tectonic history along the IPOD Japan Trench transect. *Geological Society of America Bulletin*, 93(9):829, 1982. doi: 10.1130/0016-7606(1982)93<829:asocth>2.0.co;2.

Wang, K. and Bilek, S. L. Invited review paper: Fault creep caused by subduction of rough seafloor relief. *Tectonophysics*, 610: 1–24, Jan. 2014. doi: 10.1016/j.tecto.2013.11.024.